ARTICLE

Catalytic Conversion of Biomass-Derived Polyols into Para-xylene over SiO$_2$-Modified Zeolites

Sheng-fei Wang, Ming-hui Fan, Yu-ting He, Quan-xin Li*

Department of Chemical Physics, CAS Key Laboratory of Urban Pollutant Conversion, Chinese Academy of Sciences, Anhui Key Laboratory of Biomass Clean Energy, University of Science and Technology of China, Hefei 230026, China

This work proved that biomass-based polyols (sorbitol, xylitol, erythritol, glycerol and ethanediol) were able to be converted into high-value chemical (p-xylene) by catalytic cracking of polyols, alkylation of aromatics, and the isomerization of xylenes over the SiO$_2$-modified zeolites. Compared to the conventional HZSM-5 zeolite, the SiO$_2$-containing zeolites considerably increased the selectivity and yield of p-xylene due to the reduction of external surface acidity and the narrowing of pore entrance. The influences of the methanol additive, reaction temperature, and types of polyols on the selectivity and yield of p-xylene were investigated in detail. Catalytic cracking of polyols with methanol significantly enhanced the production of p-xylene by the alkylation of toluene with methanol. The highest p-xylene yield of 10.9 C-mol% with a p-xylene/xylenes ratio of 91.1% was obtained over the 15wt%SiO$_2$/HZSM-5 catalyst. The reaction pathway for the formation of p-xylene was addressed according to the study of the key reactions and the characterization of catalysts.

Key words: Biomass-derived polyols, Para-xylene, Catalytic conversion, SiO$_2$-modified HZSM-5

I. INTRODUCTION

Biomass is the only renewable carbon source that can be used as an alternative to fossil fuel for producing bio-fuels and bio-chemicals [1]. Recently, the utilization of bio-based sugars and alcohols obtained from renewable cellulose, hemicellulose, and lignocellulosic biomass has been receiving a lot of interest [2, 3]. Especially, sorbitol (C6 polyol), xylitol (C5 polyol), and glycerol (C3 polyol) have been listed in the top 12 biomass-based building blocks [4]. Now, sorbitol (C6 polyol) is mainly produced by hydrogenation of glucose that is derived from the hydrolysis of starch. Sorbitol has been widely used in pharmaceutical, food, and cosmetic industries [5, 6]. Sorbitol has also been considered as an important renewable biomass-derived intermediate for the production of biofuels and chemicals by aqueous-phase hydrogenation and for production of bio-hydrogen through aqueous-phase reforming reactions [7–10]. Xylitol (C5 polyol), used as a sweetener and organic synthetic raw material, is mainly produced by the hydrogenation of hemicellulose or the catalytic hydrogenation of xylose [10]. Glycerol (C3 polyol) is mainly derived from the by-product in the production process of bio-diesel using oils and fats, which can be converted to 1,2-propanediol

(1,2-PDO) [11]. Erythritol (C4 polyol) is a main starting substrate for the synthesis of butanediols that are widely employed as precursors of polyester resins and polyurethanes [10]. Ethanediol (C2 polyol), which can be directly derived from cellulose, is mainly used as a precursor of polyesters such as polyethylene terephthalate (PET) [2].

Biomass-derived polyols contain high oxygen content, and the carbon atom is linked to hydroxyl group in their structure. For the production of hydrocarbon fuels and high value chemicals, the deoxygenation of biomass-derived polyols is generally required. The hydrodeoxygenation or hydrogenolysis of polyols has been proven to be a useful route for the production of fuels and chemicals from polyols [12, 13]. The process typically includes dehydration, decarbonylation, retro-aldol condensation, and hydrogenation reactions [14]. Gumina *et al.* investigated the hydrogenolysis of biomass-derived polyols (including sorbitol, xylitol, erythritol, butanediols, glycerol, 1,2-propanediol) over the Pd/Fe$_3$O$_4$ catalyst and found that lower polyols C2−C3 alcohols were formed in high yield [15]. Zhang *et al.* investigated hydrogenation and aromatization of sorbitol over Ni/HZSM-5 and the selectivity of aromatics reached 53.2% over the Ni/HZSM-5(38) catalyst [13]. Moreno *et al.* investigated the effects of temperature, hydrogen pressure, and sorbitol concentration on the performance of aqueous-phase hydrodeoxygenation (APHDO) of sorbitol with a bifunctional Pt/SiO$_2$-Al$_2$O$_3$ catalyst [16].

―――――

*Author to whom correspondence should be addressed. E-mail: liqx@ustc.edu.cn

They found that APHDO involves four fundamental reactions: (i) hydrogenation, (ii) dehydration, (iii) C−C bond cleavage by dehydrogenation and decarbonylation, and (iv) retro-aldol condensation. The main products included C1−C4 alkanes, low carbon alcohols, and carbon dioxide, and oxygen in sorbitol was mainly removed by decarbonylation and dehydration.

Alternatively, catalytic fast pyrolysis (CFP) has been considered as an effective route for producing bio-fuels and high value aromatic chemicals using biomass and its derived intermediates [17]. In CFP, biomass firstly undergoes the pyrolysis reactions in the absence of oxygen at short residence time, forming various intermediate oxygenates (*e.g.*, furans, anhydrosugars, acids, and phenolics) together with carbon oxides, water, and char as main by-products. Then the biomass-derived oxygenates can be converted into aromatics and olefins over zeolites [18, 19]. It was found that co-catalytic fast pyrolysis of cellulose and polyethylene promoted aromatic yield compared to CFP of cellulose [20]. According to the study on different biomass-based feeds, the production of aromatics increased with increasing the hydrogen to carbon effective ratio (H/C$_{eff}$ ratio) in the feeds [21]. To enhance the selectivity of target aromatics, there are several reports on the production of aromatics with modified HZSM-5 catalysts [22, 23]. It has been found that the Si-modified zeolite favored the production of *p*-xylene from furan [24]. The Ga-modified HZSM-5 increased the aromatic yield from CFP of biomass [25]. CFP is a simple technology for producing aromatics and olefins. However, the CFP process typically produces many undesirable by-products, especially coke [26]. As far as we know, there is few studies regarding selective production of *p*-xylene using biomass-derived polyols.

In this work, we showed that biomass-based polyols (sorbitol, xylitol, erythritol, glycerol, and ethanediol) were able to be converted into high-value chemical (*p*-xylene) over the SiO$_2$-modified zeolites. The effects of SiO$_2$ incorporation on the acidity and pore structural properties of zeolites were examined. The para-selectivity in the CFP of polyols was greatly enhanced using the SiO$_2$-modified zeolites by the deactivation of external surface and the adjustment of pore entrance. The influences of the methanol additive, reaction temperature, and types of polyols on the selectivity and yield of *p*-xylene in CFP of polyols were investigated in detail.

II. MATERIALS AND EXPERIMENTS

A. Materials

Polyols including sorbitol (C6 polyol), xylitol (C5 polyol), erythritol (C4 polyol), glycerol (C3 polyol), and ethanediol (C2 polyol), were purchased from Aladdin reagent. Other chemicals used were purchased from Sinopharm Chemical Reagent Company (Shanghai, China).

B. Catalysts and characterizations

HZSM-5 zeolites with the different Si/Al (25%, 50%, and 80%) were supplied from Nankai University Catalyst Co., Ltd. The SiO$_2$-modified zeolites were prepared, same as the procedures reported in our previous work [27, 28]. Briefly, the modified catalysts with the modifier of SiO$_2$ were produced by impregnating HZSM-5 with tetraethylorthosilicate (TEOS) dissolved in cyclohexane at room temperature, drying at 120 °C and calcining in air at 600 °C for 5 h. These catalysts were denoted as $x$wt%SiO$_2$/HZSM-5 (x=0−30), where x is the weight percentage of the SiO$_2$ modifier.

The BET (Brunauer-Emmet-Teller) specific surface area of the samples was tested by nitrogen isothermal adsorption in a COULTER SA 3100 analyzer, and determined by the multipoint BET method. Pore volume was calculated from the N$_2$ isotherm using the Barrett-Joyner-Halenda (BJH) method. The catalysts were also characterized by ammonia temperature programmed desorption (NH$_3$-TPD) from 100 °C to 700 °C at 10 °C/min. To examine the external acidity of the parent and SiO$_2$-modified zeolites, the cracking of 1,3,5-triisopropylbenzene (TIPB) was carried out as a surface probe reaction [29]. The probe reaction was carried out at 350 °C under atmospheric pressure at a weight hourly space velocity (WHSV) of 1 h^{-1}. Main specificities of the catalysts were presented (Table S1 in supplementary materials).

C. Catalytic conversion of polyols

The catalytic conversion of polyols were performed in a fixed-bed reactor, as described in detail elsewhere [30, 31]. Briefly, the zeolites were located in the middle of the reactor, and the reaction temperature was measured using a thermocouple inserted on the center of the catalyst bed. Before the reactions, the catalyst bed was calcined at 550 °C under air for 1 h. Then, nitrogen gas used as the carrier gas was switched to the reactor. Polyols or polyols/methanol mixtures were fed into the reactor by a syringe pump.

After reaction, the gas products were collected using an air bag, and analyzed by the GC-SP6890 gas chromatograph [32, 33]. The liquid products were trapped by the condenser, and extracted from the condenser using diethyl ether. The condensed products were weighed and analyzed by a GC-MS. The main products were quantified by the normalization method with standard samples such as benzene, toluene, xylenes, ethylbenzene, styrene, indene, naphthalene, and furan [33, 34]. To measure the coke yield, the spent catalyst was calcined at 600 °C under an air flow of 100 mL/min
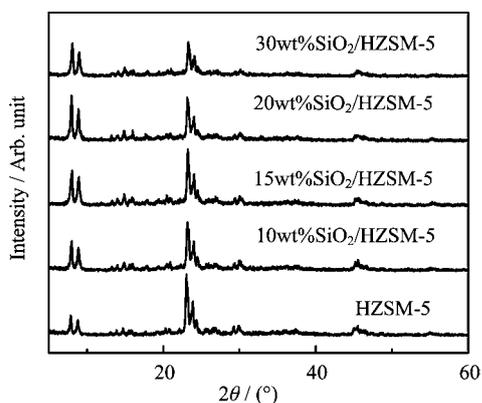
FIG. 1 XRD characterizations for the HZSM-5, 10wt%SiO$_2$/HZSM-5, 15wt%SiO$_2$/HZSM-5, 20wt%SiO$_2$/HZSM-5, and 30wt%SiO$_2$/HZSM-5 catalysts.
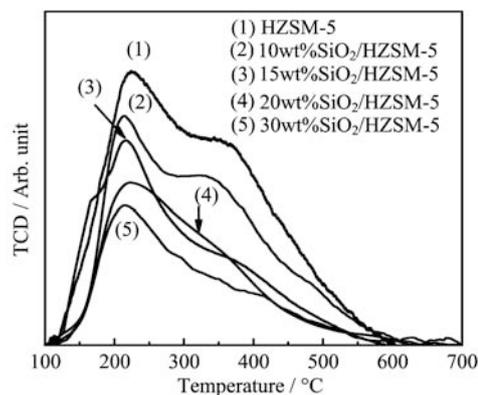

FIG. 2 Ammonia temperature programmed desorption (NH$_3$-TPD) profiles from HZSM-5, 10wt%SiO$_2$/HZSM-5, 15wt%SiO$_2$/HZSM-5, 20wt%SiO$_2$/HZSM-5, and 30wt%SiO$_2$/HZSM-5 catalysts.

for 2 h. The CO and CO$_2$ formed during this calcination were quantified by the gas chromatograph, which were calibrated by the standard gases [30]. Coke yield was obtained by the moles of CO and CO$_2$. The conversion, carbon yield, and products selectivity were calculated based on the equations described in our previous work [34, 35]. The carbon balance in all runs was over 90%.

III. RESULTS AND DISCUSSION

A. Catalyst characterizations

FIG. 1 shows X-ray diffraction (XRD) patterns of the unmodified HZSM-5 and SiO$_2$-modified HZSM-5 zeolites. The peak positions of zeolites (2θ=7.9°, 8.8°, 15.9°, 23.1°, 29.9°, and 45.5°) were not changed after the doping of SiO$_2$ even at high loading. This indicated that the structure of HZSM-5 zeolite retained without any prominent changes. There were no signals that can be assigned to the SiO$_2$ phases for the modified zeolites. This suggested that SiO$_2$ was highly dispersed on the external surfaces or pore walls of zeolites.

The BET surface area of the SiO$_2$-modified catalysts obviously decreased compared to the unmodified HZSM-5 catalyst (Table S1 in supplementary materials). A slight decrease in the micropores volume was also observed for the modified HZSM-5 zeolites. This indicates that a part of the micropores were blocked during the impregnation process, and the pore entrance of HZSM-5 zeolites could be narrowed by the modification.

FIG. 2 shows the NH$_3$-TPD profiles obtained from the HZSM-5 and SiO$_2$-modified HZSM-5 catalysts. Compared to the HZSM-5 catalyst, the acid amounts for all modified HZSM-5 were significantly reduced by loading SiO$_2$. For example, the acid amount of the parent HZSM-5(80) was 273 μmol NH$_3$/g$_{catalyst}$, but the acid amount of 15wt%SiO$_2$/HZSM-5 obviously decreased to 159 μmol NH$_3$/g$_{catalyst}$. This decrease can

be attributed to the partial coverage of external acid sites and the acid sites of the micropores.

The catalytic properties of the SiO$_2$-modified HZSM-5 were also evaluated by catalytic cracking of TIPB as a probe molecule for the external surface acid sites of HZSM-5 (FIG. S1 in supplementary materials). TIPB cannot enter the channel of HZSM-5 and only is cracked on the external surface of the catalyst [29]. It was noticed that the conversion of TIPB with the SiO$_2$-modified zeolites (*e.g.* 15wt%SiO$_2$/HZSM-5) was much less than HZSM-5, suggesting that the external active sites of modified ZSM-5 had been significantly deactivated by the treatment. The above characterization results proved that the modification by addition of SiO$_2$ considerably changed the pore structure, the acidity, and the external acid sites of zeolites. This, in turn, significantly influenced the yield and distribution of products in CFP of sorbitol, as discussed below.

B. CFP of sorbitol with SiO$_2$-modified zeolites

The types of the products obtained from the CFP of sorbitol over the SiO$_2$-loaded HZSM-5 were similar to that observed for HZSM-5 (see FIG. 3). The products can be classified into six types: aromatics, olefins, alkanes, carbon oxides (CO and CO$_2$), oxygenates (*e.g.* furan), and solid residue (coke). The main liquid products were aromatics (*e.g.* benzene, toluene, xylenes, alkylbenzenes, indenes, and naphthalenes). The sorbitol-derived oxygenates (*e.g*, isosorbide, furfural, acetol) in the liquid products were also observed over 30wt%SiO$_2$/HZSM-5.

As shown in FIG. 3, the SiO$_2$-modified catalysts significantly reduced the yields of aromatics and coke, and changed the distribution of the products obtained from CFP of sorbitol. The SiO$_2$-modified catalysts decreased the formation of polycyclic aromatics such as naphthalene, methylnaphthalene and indene. Com-
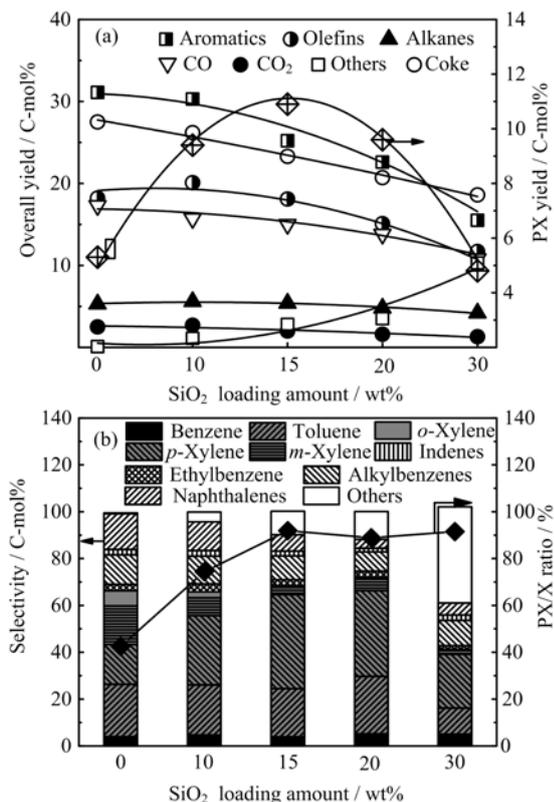
FIG. 3 Catalytic pyrolysis of sorbitol and methanol over the SiO$_2$-modified HZSM-5 catalysts with different SiO$_2$ loading amount. Reaction conditions: T=450 °C, methanol/sorbitol (molar ratio)=3/1 and WHSV=1.0 h^{-1}. (a) Overall yield and PX (*p*-xylene) yield. (b) Selectivity and PX/X (*p*-xylene/xylenes) ratio.

FIG. 4 Catalytic pyrolysis of sorbitol and methanol over the 15wt%SiO$_2$/HZSM-5 catalysts with different Si/Al ratio. Reaction conditions: T=450 °C, methanol/sorbitol (molar ratio)=3/1 and WHSV=1.0 h^{-1}. (a) Overall yield and PX (*p*-xylene) yield. (b) Selectivity and PX/X (*p*-xylene/xylenes) ratio.

pared to the unmodified HZSM-5 catalyst, the selectivity and yield of *p*-xylene using the modified zeolites were significantly improved. Among the tested catalysts, the 15wt%SiO$_2$/HZSM-5 catalyst shows the highest *p*-xylene yield of 10.9 C-mol% with high *p*-xylene/xylenes ratio of 91.1%. The improvement of *p*-xylene production can be mainly attributed to the decrease in the effective pore size of modified zeolites due to partial blockage of the pore mouth of modified zeolites and effective removal of the external acid sites [29]. Due to the pore size reduction, the formation and diffusion of *m*-xylene and *o*-xylene (with size of 7.437 Å and 7.345 Å, respectively) were more severely limited than *p*-xylene (with size of 6.701 Å) in the pore channel of the modified zeolite. This enhanced the isomerization of *m*-xylene and *o*-xylene into *p*-xylene, which then diffused out of the zeolite pores as the target product. Besides, the removal of the external acid sites inhibited the process that the *p*-xylene formed inversely isomerized to *m*-xylene and *o*-xylene on the external surface of modified zeolites [36]. Consequently, SiO$_2$-modified can significantly improve both the yield and selectivity for *p*-xylene in CFP of sorbitol.
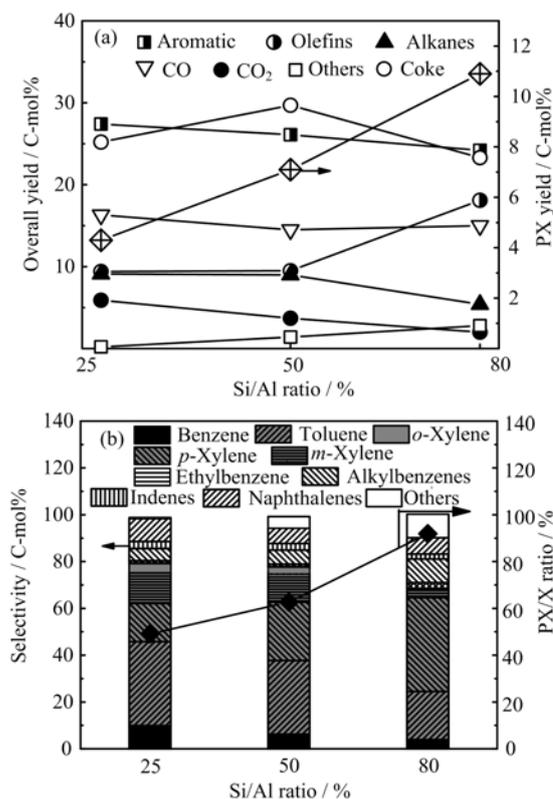
FIG. 4 shows the CFP of sorbitol over

15wt%SiO$_2$/HZSM-5 with different Si/Al ratio. The increase in the Si/Al ratio of HZSM-5 from 25% to 80% decreased the aromatics yield, since the total acidity was reduced with increasing the Si/Al ratio (Table S1 in the supplementary materials). Among the tested catalysts, the HZSM-5(25) catalyst with a Si/Al ratio of 25% exhibited the highest aromatics yield of 27.4%. With increasing the Si/Al ratio of the zeolites, the formation of CO decreased and oxygenates increased. This suggested that strong acidity favored the decarbonylation reaction and the conversion of sorbitol into aromatics. When increasing the Si/Al ratio from 25% to 80%, the selectivity of aromatics such as benzene, toluene and xylenes did not change significantly, but polycyclic aromatics such as indenes and naphthalenes slightly decreased.

C. Comparison of different polyol feedstocks

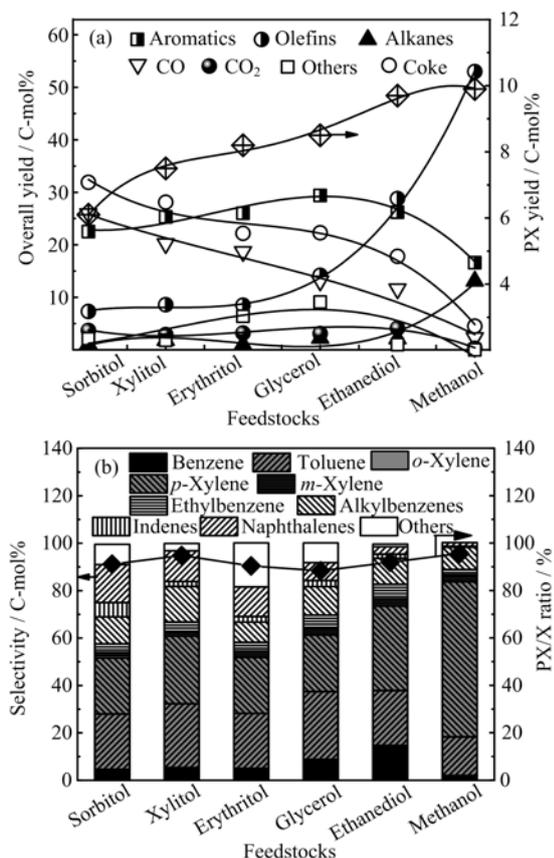FIG. 5 shows the overall carbon yield and aromatic's selectivity derived from CFP of different polyol feedstocks, including sorbitol (C$_6$H$_{14}$O$_6$,

FIG. 5 Catalytic pyrolysis of different polyols over the 15wt%SiO$_2$/HZSM-5 catalyst. Reaction conditions: T=450 °C and WHSV=1.0 h^{-1}. (a) Overall yield and PX (p-xylene) yield. (b) Selectivity and PX/X (p-xylene/xylenes) ratio.

H/C$_{eff}$ ratio=0.33), xylitol (C$_5$H$_{12}$O$_5$, H/C$_{eff}$ ratio=0.4), erythritol (C$_4$H$_{10}$O$_4$, H/C$_{eff}$ ratio=0.5), glycerol (C$_3$H$_8$O$_3$, H/C$_{eff}$ ratio=0.66), ethanediol (C$_2$H$_6$O$_2$, H/C$_{eff}$ ratio=1), and methanol (CH$_3$OH, H/C$_{eff}$ ratio=2). The total yields of aromatics and olefins decreased in the following order: methanol>ethanediol>glycerol>erythritol>xylitol> sorbitol. Compared to sorbitol, CFP of ethanediol and glycerol gave higher yield of aromatics, which was attributed to higher H/C$_{eff}$ ratio of the C2 and C3 polyols. The aromatics yield obtained from CFP of methanol was lower than that from polyols, since methanol mainly underwent methanol-to-olefin (MTO) reaction and formed olefins (ethylene, propylene and butenes) as main products, together with aromatics as main by-products. The CO yield from the conversion of sorbitol was obviously higher than that from other alcohols, indicating that sorbitol favored the decarbonylation reaction. The CFP of methanol showed the lowest coke yield as compared with CFP of other alcoholic feedstocks, since coke yields decreased with increasing H/C$_{eff}$ ratio [26].

The selectivity of aromatics for different polyols was

similar, mainly including C6−C8 aromatics (benzene, toluene and xylenes) as main aromatic products. For all polyols, the ratio of toluene to xylenes was close to 1:1, but the selectivity of benzene was much lower than toluene and xylenes. This suggests that CFP of polyols has similar reaction pathways. During CFP, these polyols underwent a series of acid-catalyzed dehydration, decarbonylation or decarboxylation reactions to form olefins, followed by the olefinic oligomerization and aromatization reactions inside the pores of zeolite to form aromatics. Unlike polyols, the catalytic conversion of methanol had the highest selectivity of xylenes (68.7%), which was attributed to the alkylation of benzene and toluene to xylenes in CFP of methanol. In addition, all polyols and methanol showed high PX/X ratio, since the p-xylene selectivity was mainly determined by the properties of the SiO$_2$-modified HZSM-5 catalyst including low external acid sites and narrowed pore entrances of zeolite.

D. Effect of reaction temperature on CFP of sorbitol

FIG. 6 shows influence of temperature on the yield and distribution of products by CFP of sorbitol over the 15wt%SiO$_2$/HZSM-5 zeolite catalyst. On increasing temperature, the yields of aromatics and coke decreased, and the gas yield including gas olefins, alkanes, CO and CO$_2$ increased. This indicates that high temperatures increased the catalytic cracking of sorbitol. In the tested reaction temperature, the main liquid products obtained from CFP of sorbitol were toluene and xylenes, with a smaller amount of benzene, ethylbenzene and other aromatics (e.g. trimethylbenzene, naphthalenes and indenes). These aromatics are formed from the catalytic cracking of sorbitol over the zeolite catalyst, similar to the production of aromatics from furans [22]. With increasing temperature, the production of xylenes decreased, and the benzene and toluene increased due to the dealkylation process of xylenes [35].

In addition, increasing the temperature tends to decrease the selectivity of both p-xylene and overall xylenes due to the catalytic cracking of xylenes. The p-xylene selectivity decreased from 40.1 C-mol% to 20.3 C-mol% from 450 °C to 600 °C. This was attributed to that the alkylation and isomerization reactions are unfavourable at high temperatures [37]. The ratio of p-xylene to xylenes was also reduced at the higher temperatures. As the temperature increased, polycyclic aromatics such as naphthalenes tended to decrease due to the reduction in the polymerization of aromatics.

E. Effect of methanol to sorbitol ratios on co-CFP of sorbitol with methanol

FIG. 7 shows the production of aromatics from co-CFP of sorbitol and methanol at different methanol to
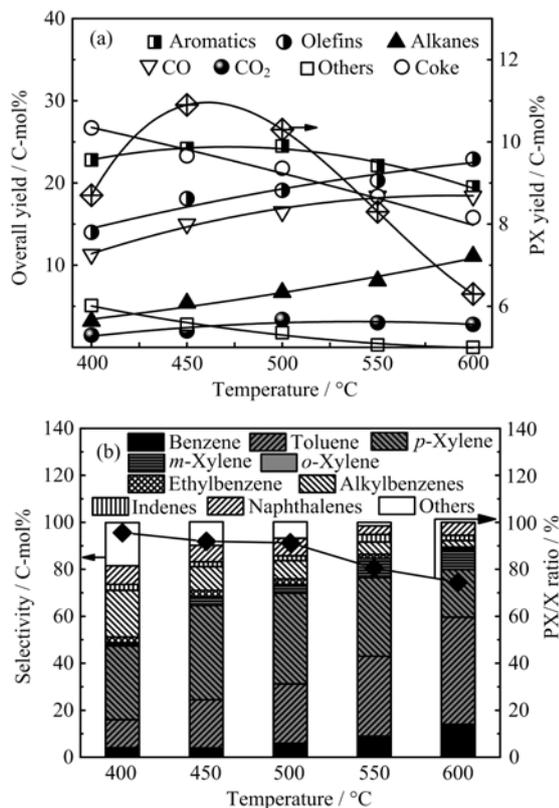
FIG. 6 Influence of temperature on the production of *p*-xylene by co-catalytic pyrolysis of sorbitol and methanol over the 15wt%SiO$_2$/HZSM-5 catalyst. Reaction conditions: methanol/sorbitol (molar ratio)=3:1 and WHSV=1.0 h^{-1}. (a) Over yield and PX (*p*-xylene) yield. (b) Selectivity and PX/X (*p*-xylene/xylenes) ratio.
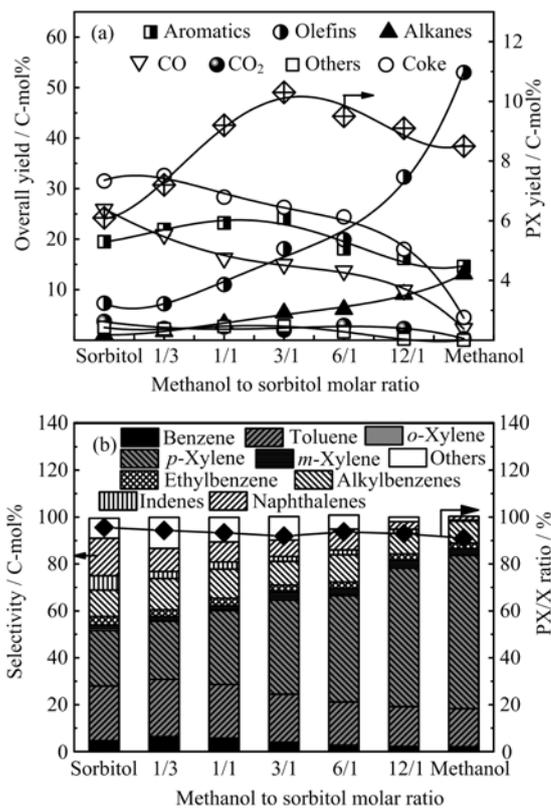
FIG. 7 Influence of methanol to sorbitol ratios on the production of *p*-xylene by the co-catalytic pyrolysis of sorbitol with methanol over the 15wt%SiO$_2$/HZSM-5catalyst. Reaction conditions: *T*=450 °C and WHSV=1.0 h^{-1}. (a) Overall yield and PX (*p*-xylene) yield. (b) Selectivity and PX/X (*p*-xylene/xylenes) ratio.

sorbitol ratios over the 15wt%SiO$_2$/HZSM-5 catalyst. Compared to CFP of sorbitol, co-feeding sorbitol with methanol considerably increased the total yield of aromatics and olefins. The maximal yield of aromatics of 24.2% was obtained at methanol to sorbitol molar ratio of 3:1. The yield of carbon oxides decreased with increasing the molar ratio of methanol to sorbitol, suggesting that more oxygen was removed by the dehydration reactions rather than the decarbonylation and decarboxylation reactions at high methanol to sorbitol molar ratio. For co-CFP of sorbitol/methanol, the coke yield also decreased due to increasing H/C$_{eff}$ ratio in the feeds.

In addition, increasing methanol to sorbitol ratios leaded to the increase in the selectivity of xylenes and the decrease of benzene and toluene selectivity, since that the alkylation reactions of benzene and/or toluene with methanol to xylenes were enhanced by adding methanol. However, the PX/X ratios are not much different and range from 91.1% to 95.6% when increasing methanol to sorbitol molar ratio from 0 to 100% in the feeds. The PX/X ratios for CFP of polyol, methanol or their mixtures were over 90% using the SiO$_2$-modified zeolites. This indicated that the PX se-

lectivity in xylenes was mainly determined by the isomerization of *m*-xylene and *o*-xylene to *p*-xylene over the SiO$_2$-modified HZSM-5 zeolites.

F. Reaction pathways

According to the above investigation, the possible reaction pathways for the production of *p*-xylene by the co-CFP of sorbitol (as a typical polyol compound) and methanol are present in FIG. 8. The catalytic conversion of sorbitol to aromatics including *p*-xylene mainly involves the following reactions: (i) the cracking and dehydration of sorbitol to lighter polyols (*e.g.*, xylitol (C5 polyol), erythritol (C4 polyol), glycerol (C3 polyol), and ethanediol (EG, C2 polyol)); (ii) acid-catalyzed decarbonylation, decarboxylation, dehydration to olefins; (iii) aromatization of olefins to mono-ring aromatics; (iv) oligomerization of aromatics to poly-ring aromatics and coke; (v) the isomerization of *m*-xylene and *o*-xylene to *p*-xylene; and (vi) the alkylation of benzene and toluene with methanol. In the absence of methanol, *p*-xylene and other aromatics were mainly formed through the reactions (Eq.(1)−(5)) during CFP
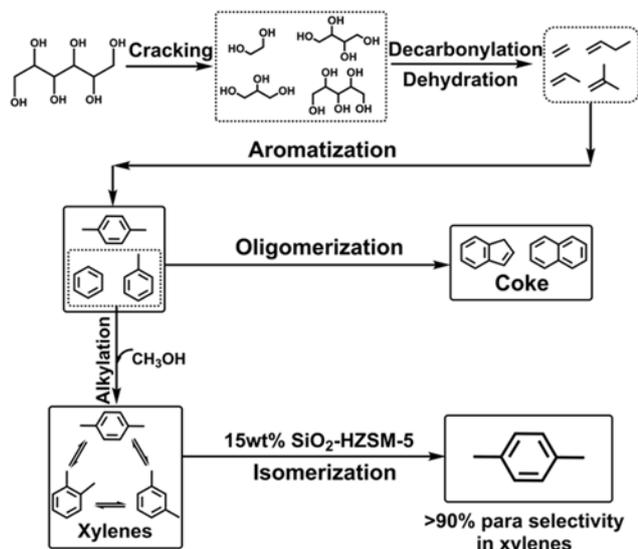
FIG. 8 Reaction pathways for the co-catalytic pyrolysis of sorbitol and methanol into p-xylene over the SiO$_2$-modified HZSM-5 catalysts.

of sorbitol.

For co-feeding methanol with sorbitol, the addition of methanol to the feed is beneficial to increase the selectivity of xylenes due to the increase in the alkylation reactions. To confirm this suggestion, the alkylation of benzene and toluene and methanol with the weight ratio of 2:1 was tested over the 15wt%SiO$_2$/HZSM-5 catalyst (FIG. S2 in supplementary materials). For the alkylation reaction of toluene with methanol, the toluene conversion was 35%, and xylenes were the main product over 15wt%SiO$_2$/HZSM-5. The selectivity of p-xylene reached about 91.1% in the alkylation reactions. High p-xylene selectivity was attributed to that the SiO$_2$-modified HZSM-5 zeolite had low external acid sites with narrowed pore entrances of zeolites. As confirmed by the results of TIPB catalytic cracking (FIG. S1 in supplementary materials), the external active sites of the SiO$_2$-modified HZSM-5 have been significantly reduced through the addition of SiO$_2$. The weak external acid sites played an important role in suppressing isomerization of p-xylene into an equilibrium ratio on the external surface of the catalyst. Benzene can also undergo the alkylation reaction with methanol and produce toluene and xylenes as main products, but alkylation reactivity of benzene was lower than that of toluene. In addition, the "hydrocarbon pool" mechanism for CFP of bio-oil was also suggested when using zeolite catalysts [38–40]. Co-CFP sorbitol with methanol may change the "hydrocarbon pool" as well as the selectivity of p-xylene. When the common HZSM-5 zeolite is used, in general, the distribution of three isomer products (p, m, o-xylene) of xylenes obtained from the methanol aromatization and toluene alkylation is usually characterized by the thermodynamic distribution (*i.e.*, the ratio of para-xylene, meta-xylene, to ortho-xylene=1:2:1) [41, 42]. In this work, it was proved that sorbitol was directionally converted into p-xylene with high yield over the modified zeolites, which the restriction of the thermodynamic distribution of three isomers was broken. The improvement in the PX selectivity was mainly due to the effective removal of the none-selective external acidic sites and the decrease in the pore size of the modified zeolites.

IV. CONCLUSION

This work presented the selective production of p-xylene from catalytic pyrolysis of biomass-derived polyols over SiO$_2$-containing MFI zeolite catalysts. The surface-modified zeolites by loading of SiO$_2$ into HZSM-5 reduced the external surface acidity and the size of pore entrance, and thus, increased the para-selectivity in xylenes from 42.5% for unmodified HZSM-5 to 91.1% for 15wt%SiO$_2$/HZSM-5 catalyst. The modified catalysts promoted the alkylation of light aromatics into xylenes and the isomerization of m-xylene and o-xylene to p-xylene. The transformation mainly involved coupling the following key reactions: the catalytic cracking of polyols, the alkylation of aromatics, and the isomerization of m-xylene and o-xylene over the surface-modified zeolites. Potentially, this process provides a useful route for the production of p-xylene using biomass-derived polyols.

V. ACKNOWLEDGEMENTS

[1] J. Pang, M. Zheng, R. Sun, A. Wang, X. Wang, and T. Zhang, Green Chem. **18**, 342 (2016).

[2] H. Kobayashi and A. Fukuoka, Green Chem. **15**, 1740 (2013).

[3] F. H. Isikgor and C. R. Becer, Poly. Chem. **6**, 4497 (2015).

[4] M. Besson, P. Gallezot, and C. Pinel, Chem. Rev. **114**, 1827 (2014).

[5] J. Zhang, J. B. Li, S. B. Wu, and Y. Liu, Ind. Eng. Chem. Res. **52**, 11799 (2013).

[6] P. A. Lazaridis, S. Karakoulia, A. Delimitis, S. M. Coman, V. I. Parvulescu, and K. S. Triantafyllidis, Catal. Today **257**, 281 (2015).

[7] J. Lee, Y. T. Kim, and G. W. Huber, Green Chem. **16**, 708 (2014).

[8] S. Qiu, T. Wang, and Y. Fang, Fuel Processing Technol. **183**, 19 (2019).

[9] Y. T. Kim, J. A. Dumesic, and G. W. Huber, J. Catal. **304**, 72 (2013).

[10] M. Grembecka, Eur. Food. Res. Technol. **241**, 1 (2015).

[11] J. J. Bozell and G. R. Petersen, Green Chem. **12**, 539 (2010).

[12] N. Li and G. W. Huber, J. Catal. **270**, 48 (2010).

[13] Q. Zhang, J. Tan, T. Wang, Q. Zhang, L. Ma, S. Qiu, and Y. Weng, Fuel **165**, 152 (2016).

[14] A. M. Ruppert, K. Weinberg, and R. Palkovits, Angew. Chem. Int. Ed. **51**, 2564 (2012).

[15] B. Gumina, F. Mauriello, R. Pietropaolo, S. Galvagno, and C. Espro, Mole. Catal. **446**, 152 (2018).

[16] B. M. Moreno, N. Li, J. Lee, G. W. Huber, and M. T. Klein, RSC Adv. **3**, 23769 (2013).

[17] R. Chang, L. Zhu, F. Jin, M. Fan, J. Liu, Q. Jia, C. Tang, and Q. Li, J. Chem. Tech. Biotechnol. **93**, 3292 (2018).

[18] W. L. Fanchiang and Y. C. Lin, Appl. Catal. A **419**, 102 (2012).

[19] J. Gou, Z. Wang, C. Li, X. Qi, V. Vattipalli, Y. T. Cheng, G. W. Huber, W. C. Conner, P. J. Dauenhauer, T. J. Mountziaris, and W. Fan, Green Chem. **19**, 3549 (2017).

[20] X. Li, H. Zhang, J. Li, L. Su, J. Zuo, S. Komarneni, and Y. Wang, Appl. Catal. A **455**, 114 (2013).

[21] H. Zhang, Y. T. Cheng, T. P. Vispute, R. Xiao, and G. W. Huber, Energy. Environ. Sci. **4**, 2297 (2011).

[22] Y. Cheng, Z. Wang, C. J. Gilbert, W. Fan, and G. W. Huber. Angew. Chem. Int. Ed. **124**, 11259 (2012).

[23] A. Zheng, Z. Zhao, S. Chang, Z. Huang, K. Zhao, H. Wu, X. Wang, F. He, and H. Li, Green Chem. **16**, 2580 (2014).

[24] Y. Cheng, Z. Wang, G. J. Gilbert, W. Fan, and G. W. Huber, Angew. Chem. Int. Ed. **51**, 11097 (2012).

[25] Y. Cheng, J. Jae, W. Fan, and G. W. Huber, Angew. Chem. Int. Ed. **51**, 1387 (2012).

[26] F. Jin, M. Fan, Q. Jia, and Q. Li, Chin. J. Chem. Phys. **30**, 348 (2017).

[27] C. Tang, L. Zhu, M. Fan, L. Zhu, and Q. Li, Chin. J. Chem. Phys. **31**, 1 (2018).

[28] Y. Zhang, M. Fan, R. Chang, and Q. Li, Chin. J. Chem. Phys. **30**, 588 (2017).

[29] J. Zhang, W. Qian, C. Kong, and F. Wei, ACS Catal. **5**, 2982 (2015).

[30] J. Liu, F. Jin, M. Fan, L. Zhu, C. Tang, R. Chang, Q. Jia, and Q. Li, Fuel **226**, 322 (2018).

[31] X. Wu, M. Fan, and Q. Li, Chin. J. Chem. Phys. **30**, 479 (2017).

[32] L. Zhu, F. Jin, M. Fan, J. Liu, R. Chang, Q. Jia, C. Tang, and Q. Li, Chem. Eng. Technol. **41**, 1027 (2018).

[33] X. Wu, P. Jiang, F. Jin, J. Liu, Y. Zhang, L. Zhu, T. Xia, K. Shao, T. Wang, and Q. Li, Fuel **188**, 205 (2017).

[34] P. Jiang, X. Wu, L. Zhu, F. Jin, J. Liu, T. Xia, T. Wang, and Q. Li, Energ. Convers. Manage. **120**, 338 (2016).

[35] Q. Jia, L. Zhu, M. Fan, and Q. Li, Chin. J. Org. Chem. **38**, 2101 (2018).

[36] G. Zhou, J. Li, Y. Yu, X. Li, Y. Wang, W. Wang, and S. Komarneni, Appl. Catal. A **487**, 45 (2014).

[37] H. Y. Liu, J. Zhu, Y. D. Wang, O. B. Yu, and T. J. Xu, Petrol. Sci. Technol. **35**, 148 (2017).

[38] S. Ilias and A. Bhan, ACS Catal. **3**, 18 (2012).

[39] S. Karnjanakom, T. Suriyaumporn, A. Bayu, S. Kongparakul, C. Samart, C. Fushimi, A. Abudula, and G. Guan, Energ. Convers. Manage. **142**, 272 (2017).

[40] K. Wang, K. H. Kim, and R. C. Brown, Green Chem. **16**, 727 (2014).

[41] D. V. Manabu, M. Mayamoto, N. Nishiyama, Y. Egashira, and K. Ueyama, J. Catal. **243**, 389 (2006).

[42] T. Wang, X. Tang, X. Huang, W. Qian, Y. Cui, X. Hui, W. Yang, and F. Wei, Catal. Today **233**, 8 (2014).